Phase diagram of a polariton laser from cryogenic to room temperature

Raphaël Butté, Jacques Levrat, Gabriel Christmann, Eric Feltin, Jean-François Carlin, and Nicolas Grandjean
École Polytechnique Fédérale de Lausanne (EPFL), Institute of Quantum Electronics and Photonics, CH-1015 Lausanne, Switzerland
(Received 29 October 2009; published 3 December 2009)

The signature of the strong-coupling regime is unambiguously evidenced in a GaN-based microcavity (MC) above the polariton lasing threshold P_{thr} at room temperature through the observation of the upper polariton branch. The MC system exhibits a renormalization of the polariton dispersion curve, namely, a reduced normal-mode splitting compared to the low-density regime. Next the dependence of P_{thr} as a function of exciton-photon detuning is investigated in the 4–340 K temperature range, which allows accessing the polariton lasing phase diagram. The observation of polariton lasing over such a broad range of temperatures reveals a clear transition from a kinetic to a thermodynamic regime with increasing temperature.

DOI: 10.1103/PhysRevB.80.233301 PACS number(s): 71.36.+c, 03.75.Nt, 71.35.Lk, 78.67.De

In recent years several features associated with high-density phases of polaritons have been reported, which were previously seen only in Bose-Einstein condensates made of ultracold atoms or in superfluid helium. If we restrict ourselves to phenomena observed under nonresonant optical excitation we can cite among others Bose-Einstein condensation of polaritons,[1,2] polariton lasing,[3–5] Bogoliubov excitations,[6] and pinned quantized vortices[7] or spontaneous polarization buildup.[8] These observations were obtained in various semiconductor microcavities (MCs) based on CdTe,[1,7] GaAs,[2,4,6] and GaN.[3,5,8] It thereby indicates that such MCs constitute an appropriate tool to study quantum effects linked to bosonic condensates in the solid state.

All these observations were made possible owing to the low effective density of states of polaritons arising from their very light mass near the center of the Brillouin zone, which acts as an energy trap in $k_{\|}$ space. Indeed, polaritons in MCs, which are admixed bosonic quasiparticles resulting from the coupling of cavity photons and excitons,[9] exhibit an effective mass up to four orders of magnitude smaller than that of excitons. However, since we deal with short-lived quasiparticles (in the picosecond range), relaxation processes of hot polaritons must be extremely efficient in order to buildup a polariton condensate at the bottom of the lower polariton branch (LPB) under incoherent (nonresonant) pumping to overcome losses due to their spontaneous radiative decay. One way to promote relaxation processes is an increase in temperature T as the exciton-phonon scattering rate should increase accordingly.

In GaN-based MCs the strong exciton-photon coupling regime (SCR) is robust at high temperatures compared to other semiconductor MCs thanks to the exciton binding energy, which can be as large as $\sim$50 meV.[10] This allowed demonstrating both polariton lasing[3,5] and spontaneous polarization buildup of a polariton condensate at room temperature (RT).[8] The robustness of GaN materials coupled to the significant progress realized in fabricating high-quality III-nitride-based MCs (Ref. 11) open new perspectives to study the properties of polariton condensates. Temperature can thus be used as an efficient and easily tunable parameter to explore and exploit the potential of such condensates.

In this Brief Report we investigate, using a GaN-based MC, properties specific to polariton condensates around the polariton lasing threshold. This includes (i) the renormalization of the dispersion curve, which exhibits a blueshift of the LPB and a redshift of the upper polariton branch (UPB), and (ii) the evolution of the polariton lasing threshold power density P_{thr} as a function of the exciton-photon detuning in the lattice temperature range 4–340 K. The latter allows extracting the phase diagram of a polariton laser and evidencing a clear transition from a kinetic to a thermodynamic regime with increasing temperature.

The sample under investigation is a 67 period $GaN/Al_{0.2}Ga_{0.8}N$ multiple quantum well (MQW) 3λ-cavity hybrid structure, which exhibits a well-resolved normal-mode splitting $\Omega_{VRS}=56$ meV in the low-excitation regime.[5,10] Angular-resolved photoluminescence (PL) measurements under nonresonant pumping were carried out in reflection geometry in a cold finger cryostat using a pulsed 266 nm Nd:YAG laser with a repetition rate of 8.52 kHz and a pulse length of 500 ps, much longer than the polariton lifetime (<1 ps). The laser beam was focused down to a 50-μm-diameter spot and incident at a fixed angle ($\theta=45°$). The emitted light was then collected using a UV optical fiber and appropriate optics offering an angular resolution of 1° and detected by a liquid N_2-cooled UV-enhanced charge-coupled-device monochromator combination.

RT angular-resolved PL spectra measured just above threshold ($P=1.1P_{thr}$) every 2° from 0° to 34° are displayed in Fig. 1(a). The first remarkable feature deals with the fact that, in addition to the LPB, the UPB is still visible at large angles, which confirms that the SCR is preserved and allows accessing the renormalized dispersion curve above threshold. The latter is reported in Fig. 1(b) together with fits based on a coupled oscillator model corresponding either to the low-excitation regime or $P=1.1P_{thr}$. It is clearly seen that the sample exhibits a reduced $\tilde{\Omega}_{VRS}=38$ meV compared to the low-excitation regime. This smaller splitting is ascribed to the combination of the blueshift of the LPB and the redshift of the UPB.[12] The latter signature is hardly accessible in other MC systems due to the strong inhibition of the PL from UPB states above threshold at low temperature, which is related to the Boltzmann occupation factor. These results indicate that in addition to polariton-polariton interactions,[13] exciton oscillator strength saturation due to Pauli exclusion does play a non-negligible role.[14] The combination of these effects is additive for the LPB whereas for the UPB the first

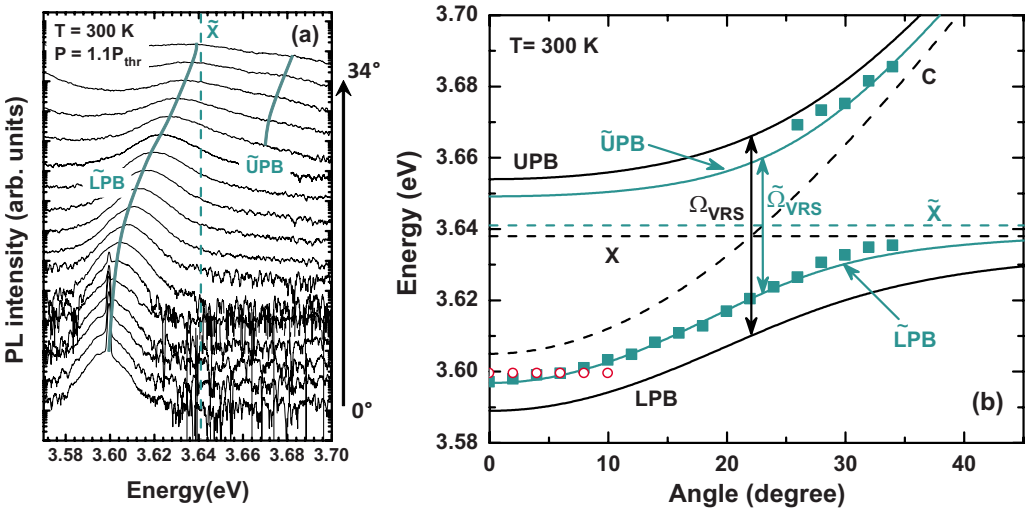

FIG. 1. (Color online) (a) RT emission spectra vs angle measured at $P=1.1P_{thr}$ every 2° and upshifted for clarity. Blue lines are a guide for the eyes showing the dispersion of polariton branches. The position of the renormalized exciton mode ($\tilde{X}$) is also reported. (b) RT experimental dispersion curve deduced from emission spectra at $P=1.1P_{thr}$ (blue squares) and fits of the LPB and the UPB in the low-excitation regime (black lines) and at $P=1.1P_{thr}$ (blue lines). The position of the emission originating from the polariton condensate (red circles) that of the uncoupled cavity mode (C) and that of the uncoupled exciton mode before (X) and after renormalization ($\tilde{X}$) is also reported (black and blue dashed lines, respectively).

one induces a blueshift and the saturation term a redshift. This behavior is well supported by the fact that the LPB blueshift Δ^{LPB} measured at in-plane wave vector $k_{\parallel}=0$ ($\Delta^{\mathrm{LPB}}\sim+7.8$ meV) exceeds the UPB redshift $\Delta^{\mathrm{UPB}}\sim-4.8$ meV, even if a quantitative estimate of the magnitude of the interaction and saturation terms [likely dependent on the renormalized exciton-cavity photon detuning δ (Ref. 15)] is beyond the scope of this Brief Report. Note that despite the pronounced LPB blueshift, the lower branch remains far from the uncoupled cavity mode (C) as at $k_{\parallel}=0$ the energy difference amounts to ~8.2 meV at $P=1.1P_{thr}$. It is also seen that the uncoupled exciton mode (X) is blueshifted by ~3 meV ($X\rightarrow\tilde{X}$) likely due to fermionic exchange interaction between polaritons explaining the slight decrease in the detuning from −33 meV well below threshold to −36 meV close to threshold.[16] We also point out that owing to the large $\tilde{\Omega}_{VRS}$ value at threshold compared with other semiconductor MCs, LPs still possess a significant excitonic character at $k_{\parallel}=0$ for negative δ of several tens of meV (i.e., when $|\delta|\leq\tilde{\Omega}_{VRS}$). For instance, the exciton fraction of LPs at $k_{\parallel}=0$ amounts to ~0.2 for the dispersion curve reported in Fig. 1(b).

Another feature worth being mentioned is the dispersionless character around $k_{\parallel}=0$ of the emission originating from the polariton condensate [Figs. 1(a) and 1(b)]. This flat dispersion extends over an angular range $\Delta\theta=\pm10°$ (to which corresponds an in-plane wave-vector spread $\Delta k_{\parallel}$). A similar feature was reported for CdTe MCs (Ref. 17) and is consistent with localization effects induced by photonic disorder. In the latter case, the polariton localization radius $r_{loc}=\Delta k_{\parallel}^{-1}$ of 1.4 μm is larger than the 0.3 μm deduced from the present measurements. This is consistent with the larger in-plane photonic disorder characteristic of III-nitride-based MCs (Ref. 18) compared with CdTe structures[17] and GaAs MCs where such a localization effect is not manifest.[2]

Following these preliminary considerations, we first studied the evolution of the polariton lasing threshold power density P_{thr} at RT as a function of δ [Fig. 2(a)]. The main feature is that the minimum of P_{thr}, P_{thr}^{min}, does not occur at zero detuning but at a δ value about −50 meV. It clearly indicates that the stimulated scattering process of polaritons, which governs polariton lasing, differs from the operation scheme of vertical cavity surface-emitting lasers,[5] the homologous structure operating in the weak-coupling regime. In the latter device, the minimum of P_{thr} occurs around zero detuning, i.e., when the spectral overlap between the cavity resonance and the gain of the lasing medium is maximum.[19] It will be shown hereafter that at RT the evolution of $P_{thr}(\delta)$ is the result of a trade off between polariton relaxation kinetics and thermal escape processes.

The evolution of the polariton lasing threshold has then been systematically investigated as a function of δ at various lattice temperatures ranging from 4 to 340 K giving access to the polariton lasing phase diagram (δ,T,P_{thr}). The corresponding data set, corrected for spatial variations in the reflectivity of the top dielectric mirror at the pump wavelength, has been converted into guides to the eyes which are displayed in Fig. 2(b) [two-dimensional (2D) (T,P_{thr}) phase diagram measured at various δ] and Fig. 3 [three-dimensional (3D) (δ,T,P_{thr}) phase diagram]. Here, we emphasize that the scatter in the data points and their scarcity for some detunings result from the strong variation in energy of the uncoupled modes over the two decades in temperature where measurements are performed. As a result it is challenging to perform measurements over a wide temperature range at a given δ. Depending on T, the accessible range of δ spans from −110 to −10 meV. Several features

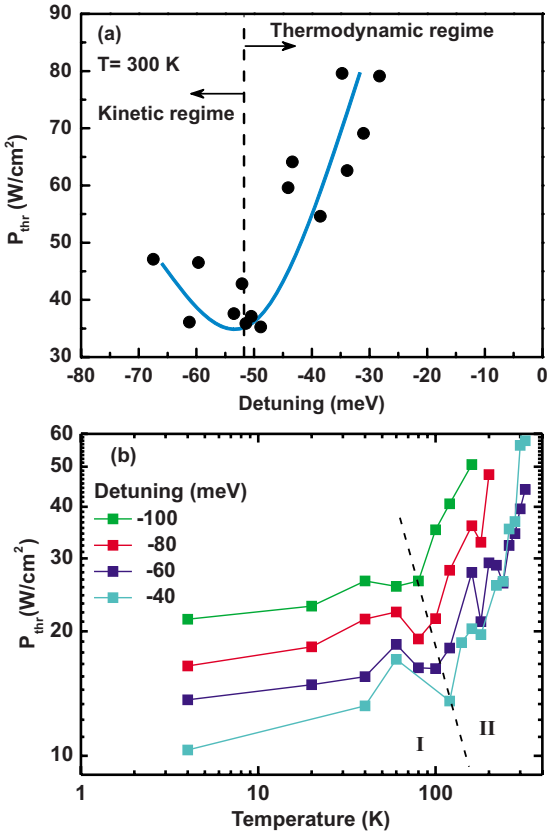

FIG. 2. (Color online) (a) Polariton lasing threshold power density (black dots) as a function of δ at RT. The blue line is a guide for the eyes. The dashed line divides the regions governed by the kinetic and the thermodynamic regimes. (b) 2D (T, P_{thr}) phase diagram measured at various δ values. The dashed line divides regions I and II (see text for details).

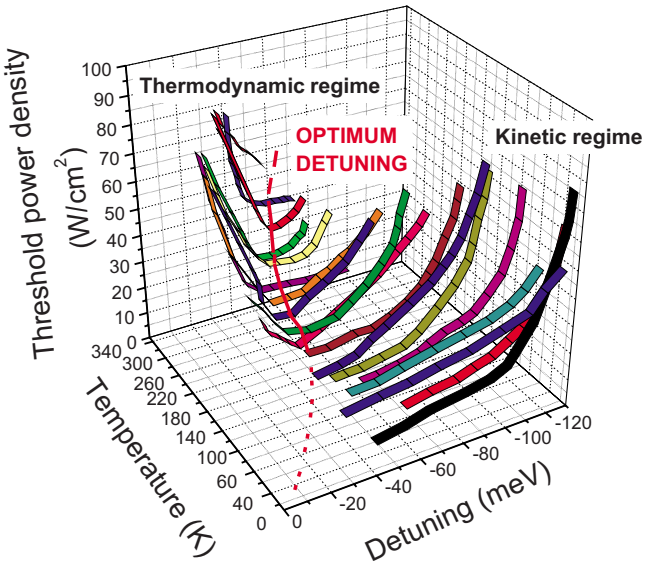

FIG. 3. (Color online) 3D (δ, T, P_{thr}) polariton lasing phase diagram. The $(\delta_{opt}, T, P_{thr}^{min})$ curve is also reported (red curve, see text for details).

are worth being mentioned: (i) for temperatures larger than 160 K a P_{thr}^{min} value is found, which does occur at negative detuning, and (ii) the larger the temperature, the larger P_{thr} at a given δ. At a given T for δ values more negative than that of P_{thr}^{min}, the P_{thr} increase is compatible with a picture where the relaxation of polaritons is dominated by the kinetics. On the other hand for smaller negative δ values the P_{thr} increase would rather correspond to a polariton relaxation process dominated by the thermodynamics as reported by Kasprzak *et al.*[20] for CdTe MCs over the temperature range of 5–40 K. This preliminary analysis is further confirmed by (T, P_{thr}) plots [Fig. 2(b)] where it is seen that at a given δ, P_{thr} is nearly independent of T in the low-temperature range (region I) whereas a transition to a temperature-dependent P_{thr} is observed at higher temperatures (region II) as theoretically predicted in Ref. 21 for various MC systems including GaN. It is also seen that for $T \leq 160$ K P_{thr}^{min} is likely to lie close to zero detuning (red short-dashed line, Fig. 3), as observed for CdTe MCs.[20] This seems to indicate that at cryogenic temperatures a trade off between polariton relaxation time τ_{rel} and polariton lifetime τ_{pol} is indeed reached near zero detuning.

The ability to observe polariton lasing over such a wide range of lattice temperatures allows exploring quite different regimes leading to the formation of polariton condensates. Thus in the $(T \geq 200$ K, $0 \geq \delta \geq -60$ meV) range the energy trap depth formed in $k_{\parallel}$ space by the LPB is close to the lattice temperature and thermal escape of polaritons from the bottom of the trap is likely to affect the buildup of polariton condensates. This is a quite unusual situation for MC systems as condensation generally occurs at temperatures where the thermal energy is significantly smaller than the trap depth.[1,2] To qualitatively account for the increase in P_{thr} with decreasing $|\delta|$ values in the above-mentioned temperature-detuning range [Fig. 2(b)], two possible thermal escape channels can be considered for polaritons lying at the bottom of the trap, namely, an intraband and an interband channel. The intraband channel involves scattering of $k_{\parallel}=0$ polaritons toward the exciton-polariton reservoir. At a given T with decreasing trap depth, LPs will be scattered much closer to the exciton-polariton reservoir, i.e., the mean diameter of the ring where $k_{\parallel}=0$ polaritons are most likely scattered at a specific thermal energy will increase. Hence much more acoustic-phonon-exciton scattering processes are required for those polaritons to relax to the bottom of the trap. Contrary to the intraband scattering process, the interband channel should be strongly temperature inhibited in our experiments due to an activation energy at least equal to the energy separation between the LPB and the UPB at $k_{\parallel}=0$. In any case in order to counterbalance this $k_{\parallel}=0$ state depopulation an increase in the pump power is needed to promote even more the power-dependent exciton-exciton (polariton) scattering processes to reach the condensation threshold.

Note that in the high-temperature range close to P_{thr} no relaxation bottleneck is observed in PL (not shown) as previously reported in bulk GaN MCs.[22] It means that polariton scattering relaxation rates, namely, those accounting for exciton-phonon and exciton-exciton (polariton) interactions, are sufficiently large to reach a quasithermal state, despite the above-mentioned thermal escape processes. Consequently, in the high-temperature range, for a given T the

dependence of $P_{thr}(\delta)$ can be summarized as follows [cf. Fig. 2(a)]: P_{thr}^{min} will result from a trade off between τ_{rel} and τ_{pol} leading to an optimum δ value, δ_{opt}, at each T. When probing detunings $\delta \geq \delta_{opt}$, the increase in the thermal escape depopulation mechanism due to the decrease in the trap depth will induce a rise of P_{thr}. On the other hand if $\delta \leq \delta_{opt}$, thermal escape is less prominent; the stronger photon character of the LPB will inhibit relaxation processes explaining the increase in P_{thr}. Now let us briefly comment the $(\delta_{opt}, T, P_{thr}^{min})$ curve displayed in Fig. 3. Above ~160 K, a progressive shift of δ_{opt} toward larger negative δ is observed with increasing T as thermal escape processes get stronger (in this regime τ_{pol} becomes a temperature-sensitive parameter). On the other hand, in region I [Fig. 2(b)] P_{thr}^{min} is expected to lie closer to zero detuning (short-dashed extension of the red curve in Fig. 3) as quoted above. It means that for practical polariton laser devices operating at RT P_{thr}^{min} would occur at negative δ values. Then, a way to further decrease P_{thr}^{min} would require an increase in the quality factor as an increase in τ_{pol} would facilitate the buildup of a macroscopic polariton population at $k_{\parallel}=0$.

Finally so far the influence of nonradiative recombinations (NRR) has been neglected though it is known they play a key role in conventional lasers, especially in systems with a large dislocation density $>1\times10^{9}$ cm^{-2}. This omission is *a priori* justified as even the largest $\frac{P_{thr}(T=300\ \mathrm{K})}{P_{thr}(T=4\ \mathrm{K})}$ ratio measured experimentally, which amounts to ~5.5 ($\delta=-40$ meV), cannot be reasonably accounted for by the decrease in the radiative efficiency of the GaN/AlGaN MQWs (a RT radiative efficiency of a few percent has been estimated from measurements performed on the bare MQW region with the same laser). This insensitivity to dislocation related NRR could be ascribed to the delocalized nature of polaritons compared with excitons or unbound electron-hole pairs.

In conclusion, renormalization of the polariton dispersion curve above the polariton lasing threshold P_{thr}, indicating a decrease in Ω_{VRS} due to both polariton-polariton interactions and exciton oscillator strength saturation, has been evidenced in a GaN/AlGaN MQW MC. The dependence of P_{thr} vs detuning in the temperature range 4–340 K has been determined, which allowed establishing (δ, T, P_{thr}) phase diagram. The latter reveals a transition from a kinetic to a thermodynamic regime with increasing temperature. Finally, the conditions leading to the optimum detuning in terms of threshold at a given temperature have been highlighted as well as the insensitivity of polariton lasers to nonradiative recombinations, making them of peculiar interest for the realization of indium free coherent light emitters.

This work was supported by the EU project Stimscat, by the NCCR Quantum Photonics, research instrument of the Swiss National Science Foundation, and by the FNS Grant No. 200020-113542. The authors acknowledge fruitful discussions with J. J. Baumberg, Le Si Dang, B. Deveaud, A. V. Kavokin, G. Malpuech, D. Sarchi, and M. S. Skolnick.

[1] J. Kasprzak *et al.*, Nature (London) **443**, 409 (2006).
[2] R. Balili *et al.*, Science **316**, 1007 (2007).
[3] S. Christopoulos *et al.*, Phys. Rev. Lett. **98**, 126405 (2007).
[4] D. Bajoni, P. Senellart, E. Wertz, I. Sagnes, A. Miard, A. Lemaître, and J. Bloch, Phys. Rev. Lett. **100**, 047401 (2008).
[5] G. Christmann *et al.*, Appl. Phys. Lett. **93**, 051102 (2008).
[6] S. Utsunomiya *et al.*, Nat. Phys. **4**, 700 (2008).
[7] K. G. Lagoudakis *et al.*, Nat. Phys. **4**, 706 (2008).
[8] J. J. Baumberg *et al.*, Phys. Rev. Lett. **101**, 136409 (2008).
[9] See, e.g., C. Weisbuch, M. Nishioka, A. Ishikawa, and Y. Arakawa, Phys. Rev. Lett. **69**, 3314 (1992); M. S. Skolnick, T. A. Fisher, and D. M. Whittaker, Semicond. Sci. Technol. **13**, 645 (1998).
[10] G. Christmann, R. Butté, E. Feltin, A. Mouti, P. A. Stadelmann, A. Castiglia, J.-F. Carlin, and N. Grandjean, Phys. Rev. B **77**, 085310 (2008).
[11] R. Butté *et al.*, J. Phys. D: Appl. Phys. **40**, 6328 (2007).
[12] Note that the collected light comes predominantly from a region of uniform excitation. This is supported by the measured reduced normal-mode splitting which would otherwise be closer or equal to its low excitation value ($\Omega_{VRS}=56$ meV) if the light was issued from a region excited well below P_{thr}.
[13] C. Ciuti, P. Schwendimann, B. Deveaud, and A. Quattropani, Phys. Rev. B **62**, R4825 (2000).
[14] D. Sarchi and V. Savona, Phys. Rev. B **75**, 115326 (2007); J. Keeling *et al.*, Semicond. Sci. Technol. **22**, R1 (2007), and references therein.
[15] The detuning is set as the energy difference at $k_{\parallel}=0$ between the position of C and that of MQW excitons. δ values have been derived from temperature-dependent measurements of materials characteristics of the sample.
[16] The peak power densities involved in the present work do not alter the refractive index of GaN (no sizeable contribution of the nonlinear Kerr term) so that the position of C remains unaffected. It was also checked that the MQW active region is not subject to screening of the quantum confined Stark effect in the range of power densities used.
[17] J. Kasprzak, R. André, L. S. Dang, I. A. Shelykh, A. V. Kavokin, Y. G. Rubo, K. V. Kavokin, and G. Malpuech, Phys. Rev. B **75**, 045326 (2007).
[18] G. Christmann *et al.*, Appl. Phys. Lett. **89**, 261101 (2006).
[19] K. D. Choquette and K. M. Geib, in *Vertical-Cavity Surface-Emitting Lasers*, edited by C. Wilmsen, H. Temkin, and L. A. Coldren (Cambridge University Press, Cambridge, 1999), p. 199.
[20] J. Kasprzak, D. D. Solnyshkov, R. André, L. S. Dang, and G. Malpuech, Phys. Rev. Lett. **101**, 146404 (2008).
[21] G. Malpuech *et al.*, Semicond. Sci. Technol. **18**, S395 (2003).
[22] F. Stokker-Cheregi *et al.*, Appl. Phys. Lett. **92**, 042119 (2008).